ISSN 0040-5795, Theoretical Foundations of Chemical Engineering, 2017, Vol. 51, No. 5, pp. 763–768. © Pleiades Publishing, Ltd., 2017.
Original Russian Text © P.S. Gordienko, I.A. Shabalin, S.B. Yarusova, A.B. Slobodyuk, S.N. Somova, 2016, published in Khimicheskaya Tekhnologiya, 2016, Vol. 17, No. 11, pp. 487–493.

TECHNOLOGY OF INORGANIC SUBSTANCES AND MATERIALS

Composition, Structure, and Morphology of Nanostructured Aluminosilicates

P. S. Gordienko[a, b], I. A. Shabalin[a], S. B. Yarusova[a, b, *], A. B. Slobodyuk[a], and S. N. Somova[a]

[a] *Institute of Chemistry, Far Eastern Branch, Russian Academy of Sciences, pr. 100-letya Vladivostoka 159, Vladivostok, 690022 Russia*

[b] *Vladivostok State University of Economics and Service, ul. Gogolya 41, Vladivostok, 690041 Russia*

**e-mail: yarusova_10@mail.ru*

Received March 14, 2016

Abstract—The data on synthesizing nanosized potassium aluminosilicates (PAS) with a ratio of Si/Al of 1–5 obtained in the $KOH–Al_2(SO_4)_3 \cdot 18H_2O–SiO_2 \cdot nH_2O–H_2O$ multicomponent system have been presented. Their composition, morphology, and IR and NMR spectra have been studied.

Keywords: synthetic potassium aluminosilicates, Si/Al ratio, NMR spectra, IR spectra

DOI: 10.1134/S0040579517050104

INTRODUCTON

Aluminosilicates of various structural types continue to find broad applications in different industrial fields, while studies of their synthesis have been under intensive development since the 1950s, as natural aluminosilicates do not always comply with the requirements to their chemical composition and properties. At present, studies of the relationships between the composition and structure of synthetic aluminosilicates and their functional properties are rather urgent. Since the functional properties of zeolites can be easily modified due to their chemical nature, this makes it possible for researchers to use them as objects in studies of the processes and mechanisms of sorption, catalysis, diffusion, and molecular sieve phenomena.

Synthetic aluminosilicates are produced by different methods, i.e., thermal, hydrothermal, and from aqueous solutions. As was mentioned in [1], one of the tasks of synthesizing zeolites with organic components consists of searching for ways to maximally simplify the process and economic solutions, but it appears reasonable to apply this approach during the selection and grounding the method of synthesizing of zeolites with any components. As was shown in [2–5], the $KAlSi_3O_8 \cdot 1.5H_2O$ synthetic aluminosilicate obtained in a multicomponent aqueous system containing silicate of the alkali metal with the specified SiO_2/K_2O ratio and aluminum sulfate consisted of agglomerates of nanosized particles of a diameter of 10–20 nm and a size of the cross section in the range of 40–70 nm. Its sorption capacity toward Cs^+ ions from aqueous solutions of cesium carbonate under static conditions without salt background that achieves the limiting theoretically possible values around 3.7 mmol/g, while the time of achieving the equilibrium concentration of cesium ions in the solution was within a few minutes (after 15 min, the degree of removal of cesium ions was 96.9%).

The objective of the present work consisted of studying the composition, morphology, and IR and NMR spectra of a series of synthetic potassium aluminosilicates (PAS) with different Si/Al ratios (1–5) obtained in the multicomponent system $KOH–Al_2(SO_3)_4 \cdot 18H_2O–SiO_2 \cdot nH_2O–H_2O$ in view of the subsequent examination of their sorption properties.

EXPERIMENTAL

Synthesis of Potassium Aluminosilicates

To obtain a series of aluminosilicates with the specified Si/Al ratio ($KAlSi_xO_y \cdot nH_2O$, where $x = 1–5$, $y = 2(x + 1)$), the following reagents were used as initial components: aluminum sulfate $Al_2(SO_4)_3 \cdot 18H_2O$ of the pure grade, potassium hydroxide of the chemically pure grade, and aqueous silicic acid $SiO_2 \cdot nH_2O$ of the analytical grade. The system components were taken in a stoichiometric ratio as calculated to produce a nonaqueous aluminosilicate with the specified Si/Al ratio. The technique of aluminosilicate synthesis is described in [2]. The formed precipitate was separated from solution by filtering using a water-jet pump, washed with distilled water, and dried at 95°C.

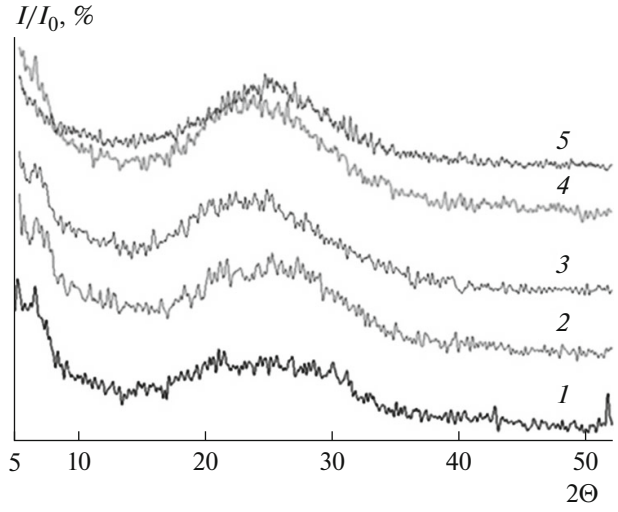

Fig. 1. Diffractograms of aluminosilicate samples with different Si/Al ratios. (*1*) 1; (*2*) 2; (*3*) 3; (*4*) 4; (*5*) 5.

Methods of Analysis

X-ray images of the precipitates were registered using a D8 Advance automatic diffractometer with the sample spinning in CuK_α radiation. The X-ray diffraction analysis (XRD) was carried out using the EVA search program with powder PDF-2 database.

For the quantitative determination of the sorbent element composition, the energy-dispersive X-ray fluorescence method with a Shimadzu EDX 800 HS spectrometer was used. The sample was ground in an agate mortar with finely dispersed Teflon (2 : 1 by weight) and placed into a mold with a diameter of 20 mm. The pellet was compacted for 2 min under a pressure of 4000 kg. The measurement time was 200 s; an X-ray tube with the rhodium anode served as an excitation source. An analysis was performed without taking into account light elements. The concentration of elements to be determined was calculated by the method of fundamental parameters using the spectrometer software. The relative measurement error did not exceed ±2%.

The sorbent thermal behavior was studied using a NETZSCH STA 449 C Jupiter device in an argon atmosphere at a heating rate of 10°C/min in the temperature range of 20–1000°C. The sorbent specific surface area was determined by the method of low-temperature nitrogen adsorption using a Sorbtometer-M device.

The IR spectra of the samples were registered in the range of 400–4000 cm^{-1} using a Shimadzu FTIR Prestige-21 Fourier-IR spectrometer at room temperature. Samples for registration were ground in an agate mortar until a finely dispersed state was achieved and deposited on a KRS-5 glass substrate in the form of a suspension in Vaseline oil. Long-wavelength IR spectra in the range of 75–500 cm^{-1} were registered using a Vertex-70v Fourier-IR spectrometer.

Studies of the samples morphological characteristics and element composition were carried out using a Hitachi S5500 high-resolution scanning electron microscope with a Thermo Scientific accessory for transmission microscopy and energy-dispersive spectrometry. ^{27}Al, ^{29}Si NMR spectra in aluminosilicate samples were registered using a Bruker Avance AV 300 NMR spectrometer (B_0 = 7 T) with magic angel spinning (MAS) technique. Registration of ^{27}AL spectra was carried out using the Hahn echo method: the diluted solution of $AlCl_3 \cdot 6H_2O$ ($[Al(H_2O)_6]^{3+}$ ion) was used as a standard. For registration of ^{29}Si spectra, the method of cross polarization of ^{28}Si-{^{1}H} with suppression of ^{29}Si–^{1}H interactions was used, while chemical shifts were counted from the signal of tetramethylsilane ($Si(CH_3)_4$). The accuracy of determining chemical shifts was 1 ppm, while that of integral intensities was ±5%.

RESULTS AND DISCUSSION

For all synthesized aluminosilicate samples, the X-ray images contain a diffuse peak in the angle range up to 35° characteristic of amorphous substances (Fig. 1). No expressed regularities are observed in the shift of the position of the peak maximum and interplane distances for aluminosilicates along with an increase in the Si/Al ratio.

Table 1 shows the data on the element composition and specific surface area of aluminosilicates, the interplane distances values calculated from the diffractogram, and general formulas with experimentally determined contents of the crystallization water calculated from the sample mass loss at its heating up to 850°C. In calculations of the quantity of crystallization water in samples, mass losses at up to 150°C were assigned to the adsorbed water (Fig. 2). Virtually all the aluminosilicate samples release water upon heating according to the same regularity, but in the case of aluminosilicate with the Si/Al ratio of 3 one observes the increased rate of water loss in the temperature range 600–650°C (Fig. 2). The maximal value of the specific surface area characterizes the aluminosilicate with the maximal silicon content (see Table 1).

In the samples IR spectra (Fig. 3), according to [6–8], one detects an intensive absorption band in the range 850–1100 cm^{-1} related to stretching vibrations of Si–O–Si and Al–O–Al bonds. Low-frequency absorption bands in the range 450–600 cm^{-1} characterize bending vibrations of Si–O–Si and Al–O–Si bonds. The absorption bands around 1600 and in the range of 3100–3650 cm^{-1} are the results of bending and stretching vibrations of the crystallization water, respectively. The maximum of the absorption band of

Table 1. Some aluminosilicate characteristics

Silicate formula	Element composition (without taking into account light elements), mass %	Specific surface area, cm^2/g	Interplane distance, Å	Molar fraction of potassium ions in 1 g of aluminosilicate, mmol
$KAlSiO_4 \cdot H_2O$	K—38.4 Al—26.3 Si—34.6	(B)*—58.3 (G)*—173.7 (m)*—0.437	3.83	5.64
$KAlSi_2O_4 \cdot 1.5H_2O$	K—36.0 Al—20.0 Si—39.8	(B)—82.4 (G)—74.5 (m)—0.0667	3.60	4.08
$KAlSi_3O_8 \cdot 1.9H_2O$	K—43.3 Al—19.0 Si—38.0	(B)—174.3 (G)—134.4 (m)—0.0831	3.82	3.19
$KAlSi_4O_{10} \cdot 2.4H_2O$	K—26.7 Al—12.2 Si—58.5	(B)—110.4 (G)—122 (м)—0.089	3.77	2.60
$KAlSi_5O_{12} \cdot 2.7H_2O$	K—24.9 Al—10.8 Si—63.3	(B)—182.8 (G)—137 (m)—0.0465	3.62	2.23

(B)* single-point BET method; (G)* comparative Gregg–Singh method; (m)* sample mass, g.

water-stretching vibrations at 3450 cm^{-1} is somewhat lower for those of free water (~3600 cm^{-1}), which is related to the presence of hydrogen bonds with the aluminosilicate crystal lattice and a cation (potassium) that compensates for the negative charge of the aluminum-oxygen tetrahedron.

Figure 4 shows the long-wavelength spectra of aluminosilicates in the frequency range of 70–550 cm^{-1}. In this frequency range, one should expect the manifestation of vibrations of both silicate crystalline base and potassium cation relative to the base [1].

In the presented spectra, one should mention insignificant changes in intensities of bands in the range of 75–170 cm^{-1} for aluminosilicates with different Si/Al ratios. To assign them to vibrations of the crystalline base or to those of potassium cations relatively to it (their concentrations change 2.5-fold (from 5.64 to 2.23 mmol) (Table 1), additional studies are necessary.

Figure 5 shows the dependences of the maxima of frequencies of peaks assigned to (a) stretching vibrations of Si–O–Si and Al–O–Al bonds and (b) bending vibrations of Si–O–Si and Al–O–Si bonds on the Si/Al ratio in aluminosilicate. As can be seen from Fig. 5, the increase in the silicon content in aluminosilicate yields an increase in the frequency of stretching and bending vibrations and the maximal values correspond to SiO_2. A characteristic feature in the silicates series with the Si/Al ratio from 1 to 5 consists of a decrease in the frequency of stretching and bending vibrations for an aluminosilicate with a Si/Al ratio equal to 3 ($KAlSi_3O_8 \cdot 1.9H_2O$) compared to the silicate with this ratio equal to 2 (see Fig. 5). For this aluminosilicate,

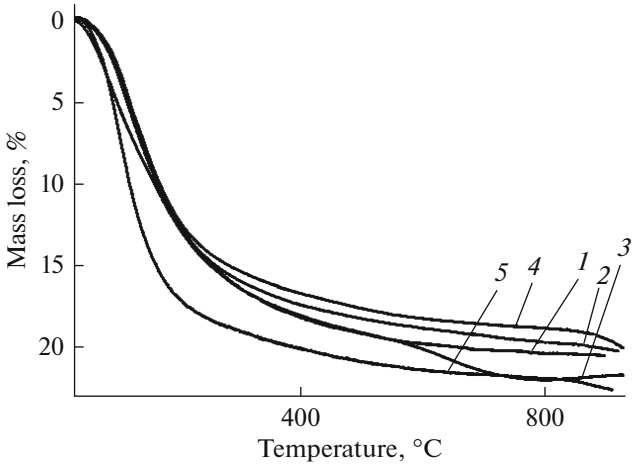

Fig. 2. Dependence of the aluminosilicate sample mass loss on temperature (Si/Al ratio: (*1*) 1; (*2*) 2; (*3*) 3; (*4*) 4; (*5*) 5).

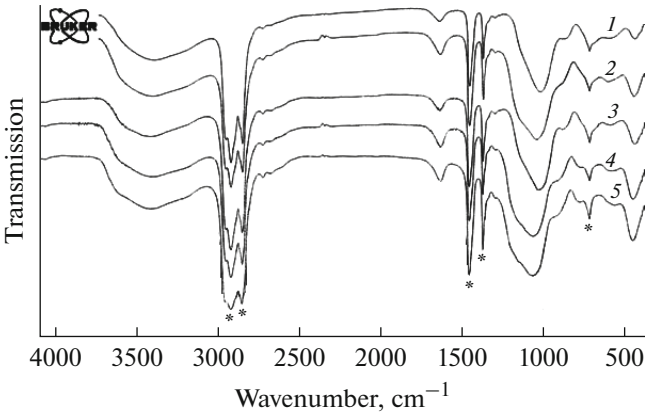

Fig. 3. IR spectra of the aluminosilicate samples with different Si/AL ratios: (*1*) 1; (*2*) 2; (*3*) 3; (*4*) 4; (*5*) 5 (*—vaseline peaks).

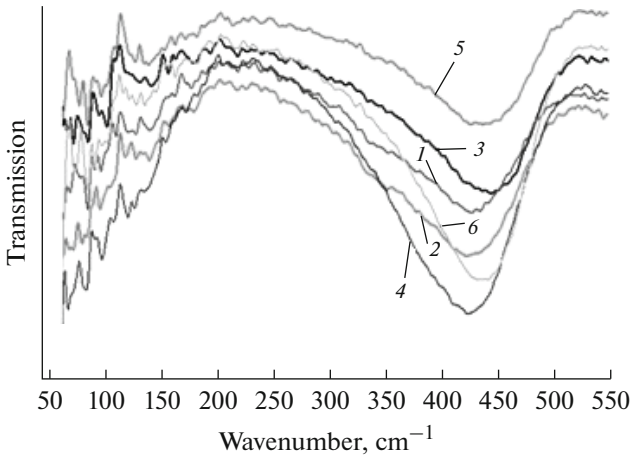

Fig. 4. Long-wavelength IR spectra of aluminosilicates with Si/Al ratios: (*1*) 1; (*2*) 2; (*3*) 2.5; (*4*) 3; (*5*) 4; (*6*) 5.

NMR spectra do not contain peaks characteristic of the octahedral coordination of oxygen by aluminum.

The morphology of all aluminosulicate samples is characterized by a multilevel porous particles structure of the pore sizes up to 100 nm (Fig. 6). Nanoparticles have the block-unit structure with unit sizes within a few nm. Aluminosilicates consist of agglomerates of spherical-like nanoparticles of a diameter in the range 10–20 nm. On the nanolevel, the morphological features of aluminosilicate particles are similar to those described in [5], independently of the Si/Al ratio.

^{27}Al NMR spectra contain signals with CS –1 to –5 and 50–52 ppm, which can be assigned to octa- and tetra-coordinated aluminum atoms, respectively [9]. The asymmetric signal shape in the spectra of $KAlSiO_4 \cdot H_2O$, $KAlSi_2O_6 \cdot 1.5H_2O$, and $KAlSi_4O_{10} \cdot 2.4H_2O$ indicates the presence of a significant electric field gradient (EFG) at the site of the location of ^{27}Al nuclei and, thus, to deviations of the local symmetry of AlO_4 and AlO_6 groups from the cubic symmetry [10]. Asymmetry emerges due to the inequality of Al–O–Al and Al–O–Si bonds and, possibly, because of the presence of hydroxyl groups in compounds. The latter is corroborated by the high intensity of signals in cross-polarization ^{29}Si NMR spectra and high values of the samples specific surface areas. Along with an increase in the aluminum concentration in the sample, the relative integral intensity of the signal assigned to octa-coordinated aluminum positions also increases, except the $KAlSi_3O_8 \cdot 1.9H_2O$ sample, in which this is hardly observed (Fig. 7, Table 2).

The silicon CS in silicates is determined by the number of silanol groups at the silicon atom and changes from –109 ppm for the SiO_4^{4-}– group (Q^4) to –91 ppm for $SiO_2(OH)_2^{2-}$– (Q^2) [11]. The presence of aluminum in the second coordination sphere also shifts the ^{29}Si NMR resonance signal to weak magnetic fields relative to the Q^4 signal [12]. In the ^{29}Si MAS NMR spectra of the studied samples, only one peak is observed, for which the chemical shift changes from –88 ppm in $KAlSiO_4 \cdot H_2O$ to –98 ppm in $KAlSi_3O_{12} \cdot 2.7H_2O$, in accordance with a decrease in the number of Si–O–Al fragments (Fig. 8).

The fine structure of spectra is absent, most likely due to the amorphous (nanocrystalline) structure of

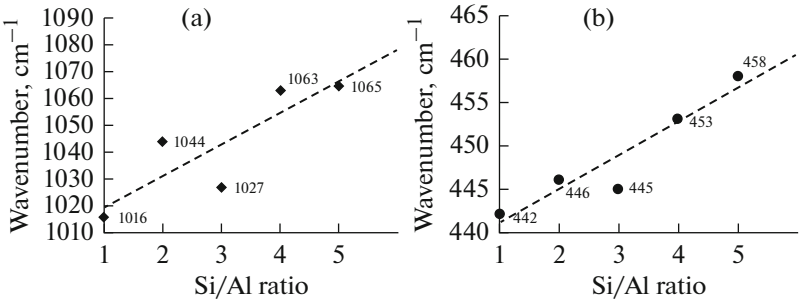

Fig. 5. Dependence of the frequency of (a) stretching and (b) bending vibrations on Si/Al ratio.

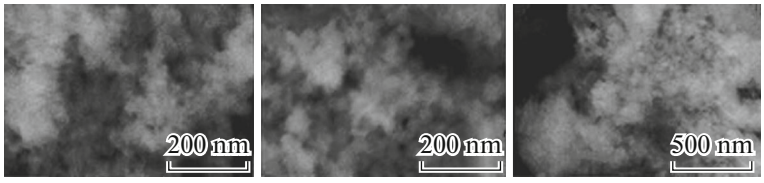

Fig. 6. SEM images of microparticles of aluminosilicate samples with different Si/Al ratios.

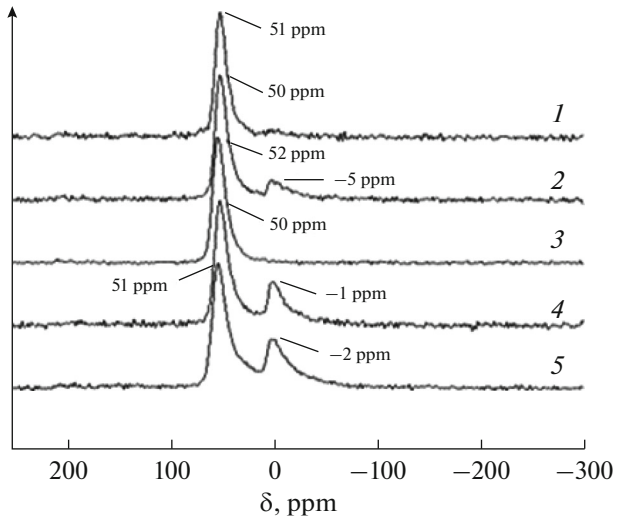

Fig. 7. ^{27}Al NMR spectra of aluminosilicates with different Si/Al ratios: (*1*) 1; (*2*) 2; (*3*) 3; (*4*) 4; (*5*) 5.

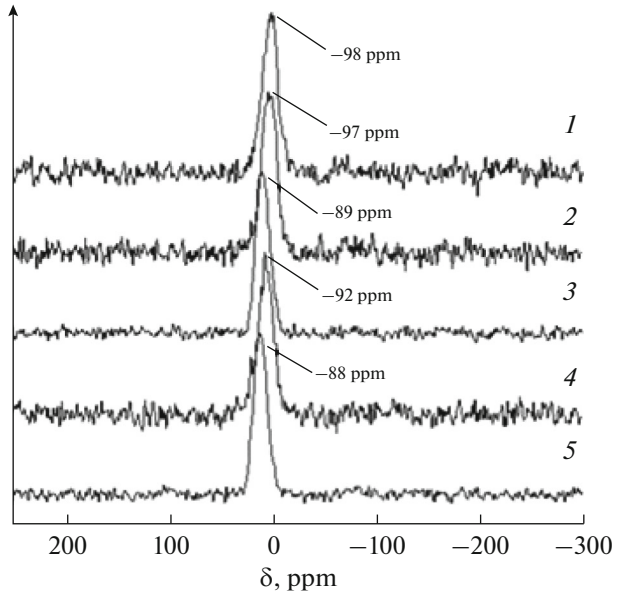

Fig. 8. ^{29}Si NMR spectra of aluminosilicates with different Si/Al ratios: (*1*) 1; (*2*) 2; (*3*) 3; (*4*) 4; (*5*) 5.

samples so that, in the structure, one observes a broad distribution of interatom distances and valence angles. As in ^{27}Al NMR, one observes a deviation in the case of $KAlSi_3O_8 \cdot 1.9H_2O$ aluminosilicate.

As can be concluded from NMR spectra, the amorphous substance contains aluminum positions with both tetrahedral and octahedral coordination.

Compared to ^{27}Al NMR spectra (Fig. 7), which characterizes the structural features of the nearest surrounding aluminum, the largest difference in CS characterize the aluminosilicate with an Si/Al ratio equal to 3, whereas in the ^{29}Si spectra, the smallest CS difference was registered as follows: –92 and –89 ppm for Si/Al ratios of 2 and 3, respectively (Fig. 8). One can assume that the nanostructural features of these aluminosilicates is related to the configurations of silicate tetrahedral also affect their sorption properties. In the series of aluminosilicates under study, the maximal sorption capacity decreases, along with an increase in the Si/Al ratio. In this series, $KAlSiO_4 \cdot H_2O$ is characterized by the presence of the maximal content of aluminum (see Fig. 7, Table 2) with octahedral oxygen coordination in structural units.

CONCLUSIONS

It has been demonstrated that all X-ray amorphous potassium aluminosilicates with Si/Al ratios of 1–5 obtained in the multicomponent system $KOH–Al_2(SO_4)_3 \cdot 18H_2O–SiO_2 \cdot nH_2O–H_2O$ consist of spherical-like nanoformations. As was found from analyzing the IR spectra, along with an increase in the Si/Al ratio, the bands of stretching and bending vibrations of Si–O–Si bonds shift to the high frequency range. As was established using ^{27}Al and ^{29}Si spectra, aluminum is present in two coordination states in the obtained series of aluminosilicates. Aluminosilicate with an Si/Al ratio equal to 3 is characterized by the presence of aluminum only in the tetrahedral oxygen surrounding. One can assume that nanostructural features of these aluminosilicates related to configuration of silicate tetrahedra also affect the sorption properties, which will be studied in subsequent works.

ACKNOWLEDGMENTS

The work was supported by the FEBRAS Program of Basic Research "Far East" (project no. 15-I-3-017) and the VSUES Program of Strategic Development.

Table 2. Areas ratios in ^{27}A NMR spectra of aluminosilicates

	$KAlSiO_4 \cdot H_2O$		$KAlSi_2O_6 \cdot 1.5H_2O$		$KAlSi_3O_8 \cdot 1.9H_2O$		$KAlSi_4O_{10} \cdot 2.4H_2O$		$KAlSi_5O_{12} \cdot 2.7H_2O$	
CS, ppm	53.3	–1.51	51.8	–1.5	53.7	44.9	52.7	–3.9	52.1	–0.5
Area, %	68	32	72	28	84	16	85	15	95	5

REFERENCES

1. Zhdanov, S.P., Khvoshchev, S.S., and Sanulevich, N.N., *Sinteticheskie tseolity* (Synthetical Zeolites), Moscow: Khimiya, 1981.
2. Gordienko, P.S., Yarusova, S.B., Bulanova, S.B., Shabalin, I.A., and Kuryavyi, V.G., Use of synthetic alumosilicate for cesium ion sorption, *Khim. Tekhnol.*, 2013, vol. 14, no. 3, pp. 185–192.
3. Gordienko, P.S., Shabalin, I.A., and Yarusova, S.B., RF Patent 2510292, *Byull. Izobret.*, 2014, no. 9.
4. Gordienko, P.S., Shabalin, I.A., and Yarusova, S.B., RF Patent 2516639, *Byull. Izobret.*, 2014, no. 9.
5. Gordienko, P.S., Yarusova, S.B., Shabalin, I.A., Zheleznov, V.V., Zarubina, N.V., and Bulanova, S.B., Sorption properties of nanostructured potassium aluminosilicate, *Radiochemistry*, 2014, vol. 56, no. 6, pp. 607–613.
6. Nakamoto, K., *Infrared Spectra of Inorganic and Coordination Compounds*, New York: Wiley, 1963.
7. Singh, B.K., Radha, T., Sumit. K., Jain, A., Tomar, B.S., and Manchanda, V.K., Sorption of ^{137}Cs, ^{133}Ba and ^{154}Eu by synthesized sodium aluminosilicate (Na-AS), *J. Hazard. Mater.*, 2010, vol. 178, nos. 1–3, pp. 771–776.
8. Plyusnina, I.I., *Infrakrasnye spektry silikatov* (Infrared Spectra of Silicates), Moscow: Mosk. Gos. Univ., 1967.
9. Fitzgerald, J., Piedra, G., Dec, S., Seger, M., and Maciel, G., Dehydration studies of a high-surface-area alumina (pseudo-boehmite) using solid-state ^{1}H and ^{27}Al NMR, *J. Am. Chem. Soc.*, 1997, vol. 119, no. 33, pp. 7832–7842.
10. Jiao, J., Kanellopoulos, J., Wang, W., Ray, S., Foerster, H., Freude, D., and Hunger, M., Characterization of framework and extra-framework aluminum species in non-hydrated zeolites Y by ^{27}Al spin-echo, high-speed MAS, and MQMAS NMR spectroscopy at $B_0 = 9{,}4$ to 17.6 T, *Phys. Chem. Chem. Phys.*, 2005, vol. 7, no. 17, pp. 3221–3226.
11. Maciel, G.E. and Sindorf, D.W., Silicon-29 NMR study of the surface of silica gel by cross polarization and magic-angle spinning, *J. Am. Chem. Soc.*, 1980, vol. 102, no. 25, pp. 7606–7607.
12. Ejeckam, R.B. and Sheriff, B.L., A ^{133}Cs, ^{29}Si, and ^{27}Al MAS NMR spectroscopic study of Cs adsorption by clay minerals: Implications for the disposal of nuclear wastes, *Can. Miner.*, 2005, vol. 43, no. 4, pp. 1131–1140.

Translated by D. Marinin